Journal of Power Sources, 42 (1993) 103–118

Calculation of potential distribution and voltage drop at electrodes on high-rate discharge: literature survey and computer-aided approach

Eberhard Meissner

VARTA Batterie AG, Research and Development Centre, D-6233 Kelkheim am Taunus (Germany)

Abstract

While the electrical resistance of the electrodes in lead/acid batteries can be neglected on low-rate discharges in comparison with other resistive contributions, the minimization of electrode resistance is an important goal to optimize high-rate performance. High electrode resistance has two undesired effects: (i) reduced cell voltage, and (ii) inhomogeneous current distribution across the electrode plane. In addition, the current inhomogeneity reduces cell voltage even more, and the electrode capacity is diminished. Using finite element analysis (FEA), potential distribution and electrode resistance are calculated even at the time of planning a new electrode geometry that employs only the technical drawing of the grid design. Unnecessary manufacture of test electrodes, only for measurement of electrode resistance and evaluation of high-rate performance, can be avoided. Consequently, electrode development and grid optimization for high-rate discharges becomes more effective, faster and less expensive.

Introduction

On discharge, a battery is operating at a voltage below the equilibrium value. At low-rate discharge, this is mainly due to the polarization of the active materials, i.e., to the overvoltages of the charge-transfer reactions, and to a concentration overvoltage in the electrolyte. But, when the discharge rate is increased, ohmic voltage losses in the current-collecting system contribute more and more, and with high-rate discharges (e.g., with uninterruptible power system (UPS) batteries, or under the cold-cranking conditions of automotive batteries), these ohmic losses may even dominate in comparison with the charge-transfer polarization.

The individual contributions of the cell components to voltage loss during discharge are depicted in Fig. 1. Top lead comprises end posts, intercell connectors, and straps of both polarities. The resistive effect within the electrode plane is the topic of this paper. The resistance of the active materials means the electronic resistance along the pathway of the current within the active material structure, i.e., from the current collector to the site of the charge-transfer reaction. The electrolyte resistance comprises the ionical resistivity and the diaphragm effect of the separator.

The path of two hypothetical units of current shall be compared: one is travelling only a short distance down the anode before it crosses over to the cathode, while the other travels much further down to the bottom of the plate before crossing over. But, the overall potential drop (ohmic and polarization) has to be the same. As the ohmic

0378-7753/93/$6.00

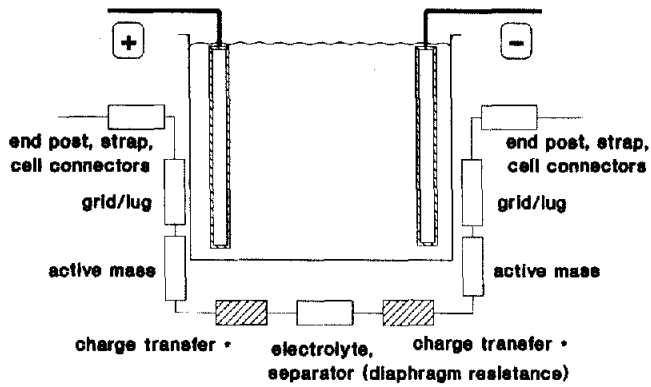

Fig. 1. Schematic of resistive contributions during discharge of a lead/acid battery; charge transfer* = non-ohmic polarization resistance.

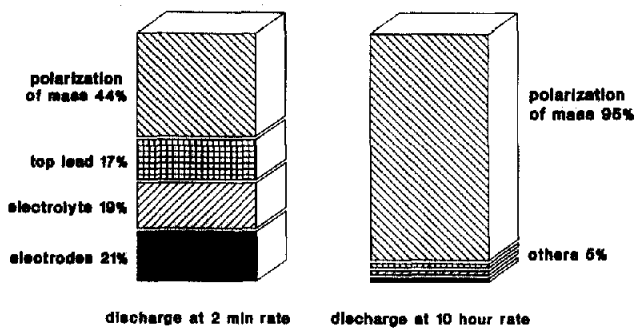

Fig. 2. Relative contribution of top lead, grids, active material, electrolyte and charge-transfer reactions to voltage drop on discharge at different rates (commercial UPS battery, 100% state-of-charge).

voltage drop in the grid is much smaller in the first path than in the second, the potential drop due to polarization has to be higher. Consequently, the current density in the upper part of the battery must be higher than in the lower part. This variation may be quite large, and may lead to a poorer discharge potential and reduced capacity of the electrode at a certain discharge rate.

While the top lead exhibits perfect ohmic behaviour, and the contribution of grids, active materials, and electrolyte are also more or less ohmic (the consequences of inhomogeneous current distribution over the electrode plane, and its dependency on the net current I, is discussed below), the resistive effect dU/di of the charge-transfer reaction is extremely non-ohmic. The latter depends on the current density i, i.e., the current per unit of active material. According to the progressive current–voltage behaviour, the differential resistivity dU_{ct}/di of the charge-transfer reaction has a rather high value at low current densities i, but decreases at higher current densities.

Therefore, the relative amounts of the different resistive contributions to the overall voltage drop depend on the current I drawn from the battery. In Fig. 2, resistive values from one battery type, discharged at two different rates, are shown. While at low rates, the ohmic portions are small and optimization of the current-collecting system will have little effect on reducing voltage losses, at high rates the relative

contribution of these components is much increased. Therefore, optimization of the current-collecting system shows promise for high-rate batteries.

Reduction of the ohmic losses in the top lead is relatively simple: the conductivity has to be improved by increasing the cross section of the current-bearing lead components, or by application of low-resistance (e.g., copper or aluminium) inserts. Both measures will increase cost, but their consequences on the ohmic losses can be calculated very simply in advance; the electrode block itself and its electrical performance is not influenced at all and, therefore, optimization with respect to the intended application is easy.

In principle, the ohmic losses in the grids can be reduced in the same manner. When the cross section of every top bar, every rib, etc., is increased by 20%, the grid's resistance will be reduced by the same percentage. But this will not only increase weight and cost, but will even change the design of the electrode block, because plate thickness and/or amount of active material have to be changed.

There is another degree of freedom that can be optimized with the grid structure, namely, the grid design. This means the relative orientation and relative cross sections of all the ribs and frame portions. In other words, the arrangement of a certain amount of current-conducting lead can be changed in such a way that the grid resistance is reduced. The following two principal qualitative rules have been established.

(i) The conductivity of the current-bearing elements in every location of the electrode should be proportional to the current flowing towards the lug in the very same place. This is the idea of tapering the frame, increasing the diameter and/or number or ribs near to the lug, etc.

(ii) The pathway from the lug to the active material should be minimal. This can be achieved by positioning the lug in the middle of the longer side of a rectangular electrode, or by usage of smaller-sized electrodes. Depending on the lug position, the electrode height-to-width ratio should not be excessive.

Theory and historical summary

The problem to be solved can be generalized as follows. Two finite (electrode) planes (extended in the x–y plane) are placed in parallel at $z=0$ and $z=d$. The space between the plates is filled with electrolyte (and separator, etc.). Current is conducted to and from the conducting planes at one point on their periphery (lug), which may be situated differently for the two planes. The current (of electrons) is distributed more or less homogeneously in the input electrode, and enters the electrolyte by a charge-transfer reaction. It is carried by ions through the electrolyte to the counter electrode, where — after another charge-transfer reaction — it is concentrated as an electron current within the electrode plane at the lug.

The goal of optimization is a maximum of homogeneity for the current-density distribution over the electrode surface (in the x–y plane) at a certain overall current. Some boundary conditions may be fixed: e.g., the height and width of the two plates and their distance apart, d; the ionic conductivity in the electrolyte/separator space; and the characteristics of the two charge-transfer reactions. On the other hand, the electronic-conducting properties in the electrode planes, and sometimes the position of the lugs, are free to be varied. The distribution of the discharge-current density in the electrode (x–y) plane, which is dealt with here, has to be clearly distinguished from the distribution in the electrode depth (in z direction), i.e., the penetration of

the current into the interior of the plate. The latter is only indirectly influenced by the afore-mentioned factors, and is not discussed here.

In principle, the problem of current-density distribution over the electrode surface can be solved by application of the algorithms of the classical theory of potential, which was developed in the 18th and early 19th centuries. As it is not only relevant for the design of batteries, but also for the huge field of galvanizing and plating, it is not surprising that the first publications came up with this topic. Kasper [1–5] published a series of papers on the theory of potential and the technical practice of electrodeposition. Applying exact mathematics, both to elementary situations and to interesting special cases such as inclined planar electrodes, line electrodes, etc., he introduced the term 'terminal effect' to describe the nonequipotential problem of resistive electrodes.

The work of Wagner [6] supplements that of Kasper by concentrating on edge problems and triangular-wave profile electrodes. The inhomogeneity of the current density was represented by the ratio of a characteristic length L to the product of the electrolyte conductivity and the derivative of electrode single potential with respect to current density. This mathematical formulation, often denoted as the 'Wagner number', is very useful for obtaining a quantitative expression of the special problem. Wagner concentrated on the case of a linear polarization curve, i.e., on a charge-transfer reaction, where the derivative of the single potential with respect to the current density is a constant, at least (as the polarization curve is a nonlinear function) within the scope of values of the distribution of current density at the actual electrode.

While most of the previous work had assumed the electrode planes to be equipotential, Tobias and Wijsman [7] took into account the electrode resistance. They extended Wagner's representation of the current-density distribution as a function of dimensionless parameters. While the exact solution was obtained in terms of infinite series, in the simple case of parallel current flow perpendicular to the electrodes, a closed form was found. With usual battery construction, this approximation is usable if the electrode distance, d, is less than 5–10% of their lateral dimension L.

Being the basis of most of the more recent publications, this work shows that the nonuniformity of the current density distribution increases, if

- the electrode resistivity increases (thinner or worse conducting electrodes at same current density)
- the electrolyte resistivity decreases (reduced electrode distance, d, highly porous separator, higher temperature)
- the slope of the polarization curve of the charge-transfer reaction with respect to the current density, dU_{ct}/di, decreases (as is usual at higher current rates)

These statements are qualitatively true in the case of both a perfect conducting counter electrode and a counter electrode of finite resistance.

In an electrolytic bath, if the current feeders are located at opposite ends of the facing electrodes, instead of at the adjoining ends, then the potential and current-density distribution is more uniform [8].

Recently, a new mathematical derivation of the whole three-dimensional problem was given [9]. Among other influences, relevant for electrodeposition on resistive substrates, the consequences of Tafel kinetics and mass-transfer limitations are discussed in ref. 10.

In 1928, Crennel and Lea [11] published measurements and calculations on the current distribution in lead/acid batteries. They perceived well the influence of electrolyte stratification and especially electrode distance. They showed that a large distance (i.e., high electrolyte resistance) reduces the effect of electrode resistance, and may even

lead to a maximum of current density at the bottom of the electrode, when an electrolyte reservoir is located there. These authors appear to be the first to have measured an electrode resistance, and to have dealt with the quasi one-dimensional electrode (i.e., width $\ll$ height, in that special case 1:3) in order to simplify the situation to a two-dimensional problem in the x–z plane. They calculated an initial ratio of 1:2.7 of the current density at the bottom and the top of the plate, when a plate of 77.5 cm height was discharged at the 8-h rate (6 mA cm^{-2}).

The work of Tobias and Wijsman [7] was later applied by Shepherd [12] to the situation of a battery. In a subsequent publication [13], he stressed the important case of $d/L \ll 1$ (i.e., electrode distance is small with respect to the electrode lateral extension), and described a battery analog consisting of silver electrodes and mercury to model a cell without polarization overvoltage. Perfect agreement was obtained with the mathematical prediction. In the case of $d/L \ll 1$, there is virtually no influence of this ratio on the current distribution [14].

Besides many publications on the behaviour of porous electrodes, especially by Euler *et al.* [15], some work on the current distribution was performed in the 1960s and 1970s at VARTA's central laboratory. From a calculation of the current distribution over the height of tubular electrodes [15], the limitation of electrode height, especially at high rates, was clearly demonstrated. The consequence was the development of the 'Double-decker' cell, i.e., the two-story construction for tall submarine cells. A series of papers deals with an autoradiographical investigation of the inhomogeneous active-mass utilization [16]. In ref. 17, a method for evaluation of the effective electric resistance of the grids of lead/acid batteries is described; it assumes a homogeneous current density over the electrode surface. Euler introduced a figure-of-merit to compare different grid designs, and discussed the influence of grid area. The mutual influence of the two electrodes was pointed out. In ref. 18, the principles of grid optimization with respect to electric-vehicle batteries were described and quantified. The influence of electrode size, lug position, and especially grid design (i.e., strengthening and tapering of top bar, orientation of ribs towards the lug, distribution of conducting lead proportional to the local current, etc.) was examined, and an estimation was made of the inhomogeneity of the current distribution.

The improvement of voltage and capacity by increasing the electrode conductivity of high plates was demonstrated by Bagshaw *et al.* [19].

Puzey and Orriel [20] were the first to treat battery electrodes as two-dimensional structures. They measured equipotential lines on positive and negative pasted electrodes on discharge and charge. By design improvements, the influence of the grid design and the position of the lug was demonstrated. With discharge, the equipotential curves moved towards the lug in the case of the negative electrode, which showed a contribution of the negative active material to the electrode conductivity. No such effect was found with the positive electrode. The distance of the two electrodes seems to have been quite large (no data were given in the paper), as the counter electrode was found to exert very little effect on the potential distribution.

In the last two decades, several mathematical models to simulate potential — and even current — distribution have been developed. The calculated results have been compared with experimental data by several authors. Sometimes only the behaviour of the pure grid is determined [21], but in other cases the conductivity of the active material on the potential distribution is also taken into account [22–24].

Frequently, the complexity of the three-dimensional problem is reduced to a two-dimensional model. In one approach, only the situation in the electrode plane is examined, influences of polarization, electrolyte resistance, and counter electrode are

neglected, and the approximation of homogeneous current distribution is used; while in an alternative approach, the width of the electrode is ignored, i.e., only electrode height h, the distance d of the two electrodes, and the inhomogeneity of the current density are considered.

Several papers deal with the approach of homogeneous current density [21, 24, 25]. Experimental data obtained by immersing grids in electrolyte and evolving oxygen or hydrogen at these surfaces at considerable rates (i.e., at high polarization) correspond to this condition. This is not always equivalent to the situation in a battery, where the distribution of active material, and not of the grid surface, is relevant for current distribution, *v.i.*

Usually, classical regular orthogonal grids have been simulated [21, 24, 26] or a homogeneous isotropic-conducting electrode has been analyzed [25]. The influence of the height-to-width ratio of the plates has been investigated [24, 25]. The effect of optimization was presented by two types of changes: (i) shift of the position of the lug [21, 24, 25], or the introduction of several tabs [24, 27]; (ii) redistribution of the conducting material at constant overall weight of the grid, i.e., increase of the cross section of ribs near to the lug, while others were reduced [21].

The second two-dimensional approach, that ignores the electrode width but considers inhomogeneous current density [28, 29], already reveals some consequences of the restricting boundary condition of homogeneous current-density distribution, which becomes clear in a full three-dimensional model. According to Le Chatelier's principle of least restraint, for the same total electrode current, the potential distribution is found to be more uniform when the current density is inhomogeneous as opposed to uniform [18, 22, 23]. If the current feeders are located at opposite ends of the facing electrodes, instead of at the adjoining ends, the potential- and current-density distribution is more uniform [8, 18], but the cell resistance (in the fully-charged state) is increased [18, 27]. The initial voltage of such a cell would be somewhat lower, but the discharge curve would be less steep, and the available capacity would be increased because of the more homogeneous utilization of the positive active material.

When the time dependence of polarization of the electrodes, changes of electrolyte concentration, temperature, etc., are also taken into account, the changes of potential- and current-distribution during discharge, and the inhomogeneity of the active material utilization, can be calculated [23]. The current-density distribution becomes more and more homogeneous during discharge, as the change of acid concentration has an equilibrating effect [23, 28]. This reduction of inhomogeneity with proceeding discharge, and sometimes even a reversal (i.e., higher current density at the bottom than at the top of the electrodes at the end of discharge), has also been found experimentally [24, 26, 30, 31]. Altogether, from sophisticated models, the discharge-voltage curve can be calculated [23, 31–35]. In some models, even the effect of acid stratification is considered [35].

Vaaler and Brooman [30] applied their three-dimensional model for electrolysis [36] to batteries with orthogonal grids. The conductivity of the active material was taken into account, but the polarization was not. In a more recent paper, all these contributions were considered [26], and several proposals were made to shift the position of the lug and to improve the rib conductivity near to the lug, similar to ref. 18.

In a series of papers, Meiwes [37–41] measured the current-density distribution in different batteries, and developed semi-empirical models. His elementary statement, that one point on the electrode surface exists which is representative for the whole electrode, i.e., which shows average behaviour [38], is of fundamental importance: to

know the current behaviour at this point means to know the overall behaviour of the electrode.

Figures-of-merit to compare experimentally different grid designs, similar to Euler [17], were defined by Valeriote [42]. He described different experimental methods to evaluate grid designs. Unfortunately, the more significant methods are quite expensive with respect to time and apparatus. Moreover, an electrode has to be physically realized, before its performance can be investigated according to the proposed methods; quick analysis of intended changes of design, without making a grid or even an electrode, are not possible.

Therefore, grid-design optimization is an ideal field for mathematical simulations. In contrast to any experimental method, an actual electrode is not needed to evaluate the electrical performance. These methods have been proven to be a powerful means for analysing the potential- and current-density distribution, and to compare different grid designs (*v.s.*). Nevertheless, all these models use 'unit cells' for the discretisation of the electrode plane, which depend on the geometry of the grid network, and seem to be very cumbersome with respect to adaption to other, especially nonorthogonal and nonuniform, grid designs. In ref. 43, for example, diagonal grid elements are approximated by a 'staircase' of vertical and horizontal elements.

It was the goal of our studies to develop a tool that gives a figure-of-merit to compare all different grid designs, and that is easy to use, not only by the specialist, but also by the common product designer. The information contained in the computer-aided design (CAD) should be sufficient to obtain the consequences of a special design change within minutes; no hardware for production means like moulds, etc., and no experiments should be necessary.

Method

A computer program package was developed, which directly fits to the CAD system, where new grids are developed. When the grid is designed as usual, the CAD drawing already contains all information about the resistance of this projected grid — it has just to be used!

A specially designed MACRO program extracts the data that are relevant for the computation of the grid's resistance (e.g., grid size, lug position, coordinates of ribs, thickness of frames, cross sections, etc.) directly from the CAD database and stores them on file. These data are used by another program to create a BATCH file to control a commercial finite element analysis (FEA) program. The finite element method considers a solid continuous structure as an assemblage of discrete pieces, called elements, that are connected together at a finite number of points or nodes. While in the real structure, the number of interconnecting nodes is infinite and the size of the elements is infinitely small, in the model, the structure is decomposed into macroscopical two- or three-dimensional elements. This is analysed in a procedure similar to that used in structural analysis beam theory. The problem is solved exactly at the nodes, while the stresses within the elements are obtained by interpolation of the node values. If the decomposition is suitably performed, mathematics will approximate the reality quite well and within reasonable computation time. Therefore, decomposition is one of the most important steps of FEA to find a compromise of exactness and expense.

Today, FEA is a common and powerful tool in many technical and scientific areas. Commercial program packages are available for mechanical, electrical, magnetical

and thermal problems, and their superpositions, as well for stationary or dynamic problems. Special skilled and experienced staff are necessary to make use of these programs. As the potential distribution on the electrode surface is quite a simple two-dimensional stationary problem, the analysis may run in BATCH mode without any need for human intervention.

The BATCH file to control the FEA program comprises all commands for the FEA program to set up the model of the grid, to define material parameters and boundary conditions (preprocessing), to run the solution routine to compute the potential distribution in the electrode plane, and to give the calculated potential data to file, terminal and plotter (postprocessing). Therefore, the designer has not to deal with the FEA, which is completely running in the background.

From the potential data written to file, a further program calculates the value of the effective grid resistance R_{eff}. The result is written both to file and to terminal. This value and the potential distribution pattern (shown on terminal and plotter) are the only quantities with which the designer has to deal. By variation of design and comparison of the calculated results, the sensitive design details are traced and optimized. Superfluous portions of the structure can be reduced easily.

In Fig. 3, a schematic flow chart of the design optimization process is visualized. Iteratively, the designer modifies the grid, guided by the calculated R_{eff} value and the plotted potential distribution with respect to electric properties, and his/her own personal experience with respect to manufacturing criteria.

In Fig. 4, an example of the modelling of a standard automotive battery diagonal grid within the preprocessing step of the FEA program is shown. Frame and lug are simulated as an assemblage of two-dimensional, four-node isoparametric solids. The suitable dissection is done automatically by the program that defines the BATCH file. The ribs are simulated as two-node conducting bars, connecting intersections and junctions of ribs. This was found to be an adequate compromise between, on the one hand, exactness of the model and of the results, and of computation time on the other hand.

As a boundary condition of the model, the current is introduced homogeneously over the active-material surface, i.e., every pellet has to bear a current proportional

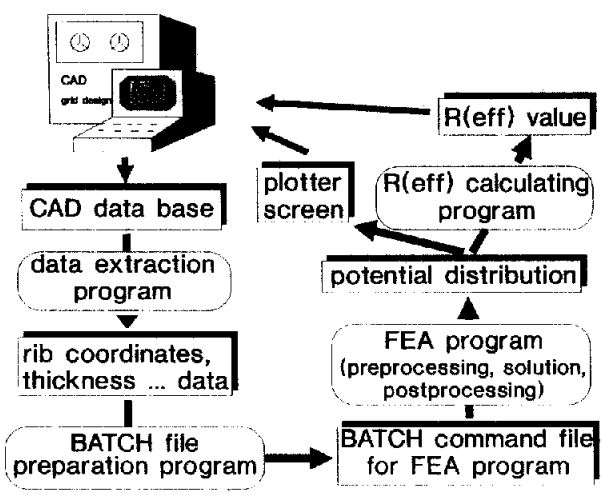

Fig. 3. Flow chart of grid-optimization process.

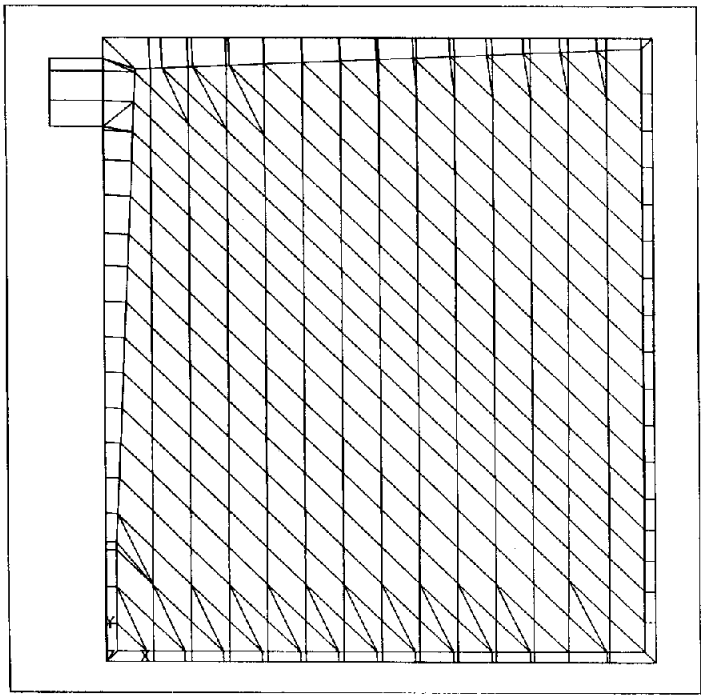

Fig. 4. Model of standard diagonal automotive battery electrode from finite elemental analysis (FEA) preprocessing.

to its surface in the electrode plane. No current is introduced to the frame and the lug surface. The sink for the current is the upper edge of the lug, where the potential value is fixed to zero as a further boundary condition.

The assumption of homogeneous current density perpendicular to the electrode plane is an approximation (*v.s.*) that is true to within about 10% for modern automotive electrodes, even under cold-cranking conditions (estimated according to ref. 18). With this approximation, the influence of electrode resistance on cell voltage at the very beginning of high-rate discharge is somewhat overestimated. On the other hand, as low electrode resistance leads to a less steep discharge–voltage curve, the results within this approximation give suitable information for the cell voltage after 30 s of cold-cranking discharge according to the DIN standard.

The above approximation of homogeneous current density in the pellets is much better than the simple experimental methods, where the whole current is directed from the lug to the opposite corner or the lower edge of the frame [17, 42]. It is similar to experiments, where hydrogen is evolved at a polarized grid that is suspended in an electrolytic bath. But in this case, the current density is not proportional to the amount of active material (that is relevant for the electrode performance), but to the free surface of the grid structure. Much hydrogen is evolved at the frame surface. Only with grids having uniform pellet size and little frame surface (e.g., expanded metal [42]) will hydrogen evolution give a current distribution that is approximately proportional to the amount of active mass.

The conductivity of the grid elements depends on the lead alloy used. This dependency [44, 45] has to be taken into account if an exact prediction of the grid

resistivity is required. Arbitrary conductivity values can be used, when only relative resistance changes as consequence of changes in design are to be compared.

Optionally, the conductivity of the active masses in the pellets can be taken into account. Triangular or quadrilateral shaped pellets are simulated as two-dimensional, three- or four-node isoparametric solids, bordered by the ribs. Pellets with 5 or more corners are modelled as an assemblage of such elements (cf., Fig. 4). A suitable dissection is again performed automatically by the program. The conductivity of these mass elements is chosen in accordance with the thickness of the pellets (which may be different from the grid) and the polarity of the mass. Positive active-material conductivity is about 135 Ω^{-1} cm^{-1} [46, 47]. The conductivity depends on the deviation δ from stoichiometry of $PbO_{2-\delta}$ [48]. According to the poor conductivity of the positive mass with respect to the lead grid (pure lead is $\sim$48000 Ω^{-1} cm^{-1}), the positive active material contributes little to the electrode conductivity, i.e., pasted electrode and pure grid show nearly the same potential distribution [20].

On the other hand, as the conductivity of the charged negative active mass is much better ($\sim$5000 Ω^{-1} cm^{-1} [46]), its contribution to the electrode conductivity cannot be neglected.

With this model (cf., Fig. 4) and the boundary conditions mentioned above, the FEA program calculates the potential distribution in the electrode plane. This is plotted in Fig. 5. Near to the lug, the current of the whole electrode becomes concentrated and the equipotential curves are close together according to the high current density

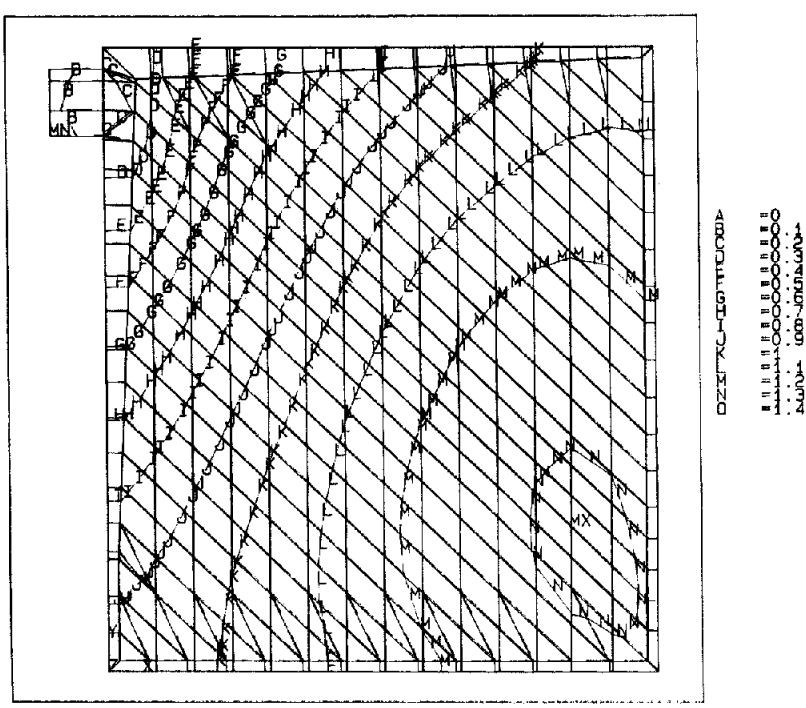

Fig. 5. Potential distribution over the surface of the diagonal grid automotive electrode according to Fig. 4, when a current $I=1$ A is assumed to flow uniformly across the active-mass areas.

within the electrode plane. Far away from the lug, the current density within the plane is much lower, and the distance of the equipotential curves is greater.

The maximum of the potential distribution is usually not in the grid corner opposite to the lug, but within the mesh of the ribs because the cross section of the frame is usually greater than that of the ribs, i.e., the corner itself is in relatively good electronic connection with the lug. From this potential distribution, the effective electrode resistance R_{eff} is calculated as the average of the potential values within the pellets (i.e., the active material, not the frame and lug), divided by the overall current. According to the statement of Meiwes [38], *vs.*, this is just the resistance from the lug to the representative point on the electrode surface. If all the current I travels via this point, instead of spreading over the electrode plane, then the voltage drop in the electrode is: $\delta U = IR_{\text{eff}}$.

Instead of a complex electrical network of resistors in the electrode plane, and perpendicular to it in the electrolyte to the counter electrode in accordance with the many different pathways of the current spreading over the electrode plane, this simple equivalent circuit diagram consists only of R_{eff} in the electrode plane, and R_{elyt} that represents the electrolyte resistance.

As the potential at the upper edge of the lug is set to zero as a boundary condition of the problem, the resistivity of the lug is included in R_{eff}. In this manner, not only the position of the lug but also its width and thickness are taken into account. The value of $R_{\text{eff}} = 0.99$ mΩ, calculated from the potential distribution shown in Fig. 5, means that at a cold-cranking current of 50 A per plate, the voltage drop at this grid will be about 50 mV.

Figure-of-merit and examples

The most important advantage of this approach to calculate electrode resistivity is its flexibility. There are no restrictions to a special type of grid pattern. Any grid design can be studied, when it is sketched with the CAD system.

Figure 6 shows the potential distribution at a conventional orthogonal grid with the lug placed right in the corner. When the calculated R_{eff} values are compared, the grid weight has to be taken into account: the goal is not to minimize R_{eff} alone, but to do this with low grid weight G. Therefore, the figure: $Q = (GR_{\text{eff}})^{-1}$ can be used as a figure-of-merit for a grid of a special size to be pasted with a special amount of active material. Q has to be brought to a maximum, while the grid designer has to observe the manufactural criteria. These criteria usually represent the practical limits for optimization of the design of cast grids. Electrodes with a different size or a different amount of active material should not be compared using this figure-of-merit, as smaller electrodes of same design have principly higher Q values than larger ones (cf., [18]).

With expanded grids, there are less degrees of freedom that can be optimized with respect to cast grids. Nevertheless, the size and orientation of the diamonds, together with the rib diameter, can be chosen according to the special application. As an example of easy 'what, where, if...'-analysis, Figs. 7 to 9 show the influence of the lug position with the same expanded grid. The shift of the lug with the CAD system takes the designer only seconds, and the computer several minutes, to calculate the new potential distribution and the R_{eff} value.

With this example, the R_{eff} value is markedly reduced from 2.44 mΩ, through 1.89 mΩ, to 1.65 mΩ, when the lug position is shifted towards the centre of the plate.

In the same quick manner, the consequences of positive grid corrosion on electrode performance can be estimated, if some assumptions about the corrosion mechanism

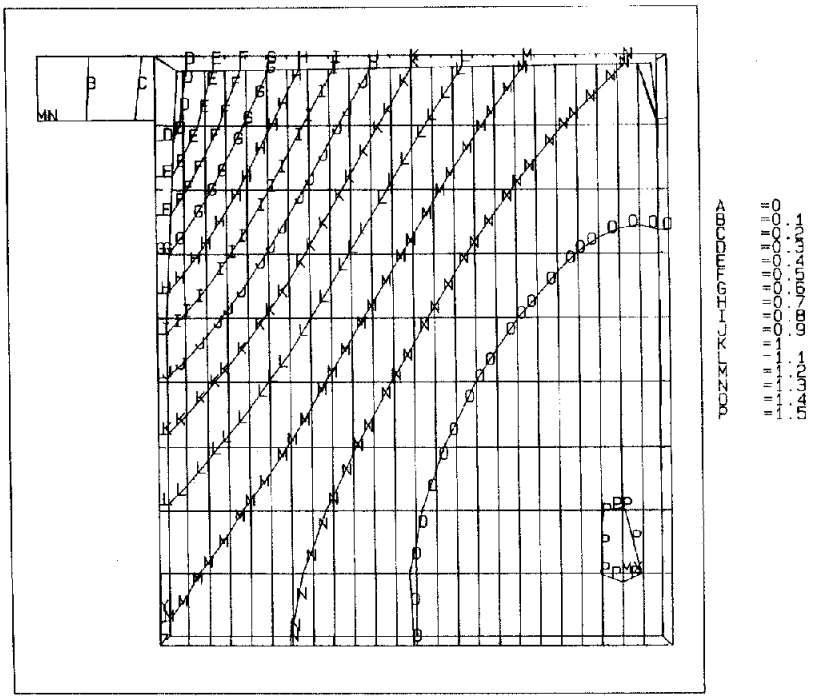

Fig. 6. Potential distribution over the surface of an orthogonal grid automotive electrode.

is made. If corrosion is assumed to attack each lead surface in the same manner, thin structures will be attacked relatively more than thicker ones. This will lead to a change of the potential pattern, if the grid consists of elements of different thickness. Therefore, a forecast of some aspects of the performance after a period of duty of the battery is possible.

Conclusions

Optimization of grid design, i.e., efficient arrangement of grid ribs and economic choice of cross sections of ribs and frame, is a promising goal to improve energy and power density, especially for batteries discharged at high rates. Reduction of the grid resistance has two favourable consequences:

(i) the ohmic voltage drop on the grid structure is reduced, and thus causes higher discharge voltage, less heat evolution, and even higher capacity, when the battery is discharged to the same end-of-discharge voltage;

(ii) the discharge current is distributed more homogeneously over the electrode plane, which leads to a more flat discharge curve and even increases — according to Peukert's law — in the beneficial effects mentioned above; beyond this, more uniform current density leads to more uniform active-material utilization, which improves cycle life.

Optimization means an arrangement where the grid resistance is minimized by intelligent rearrangement of a certain amount of current-conducting lead, or, vice

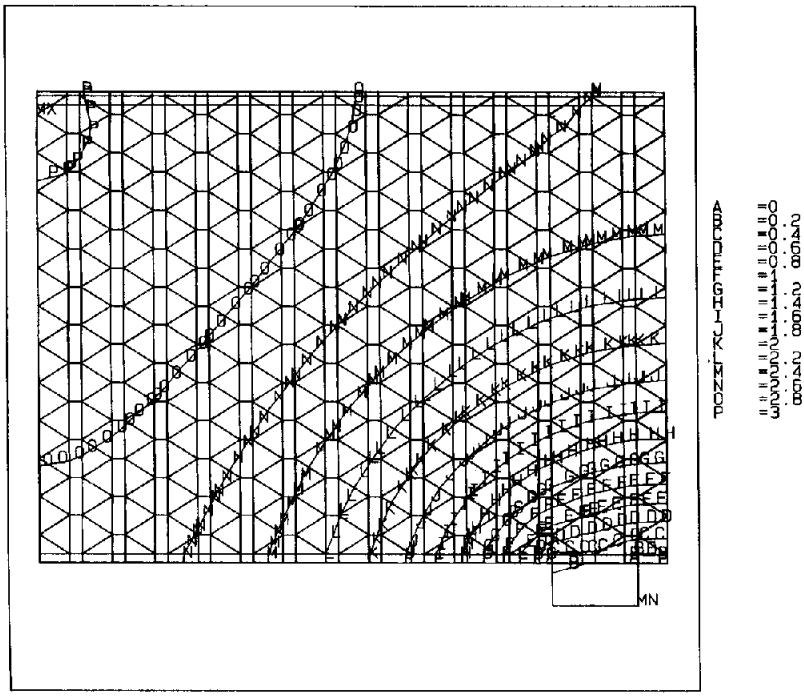

Fig. 7. Potential distribution over the surface of an expanded grid with lug near to the corner.

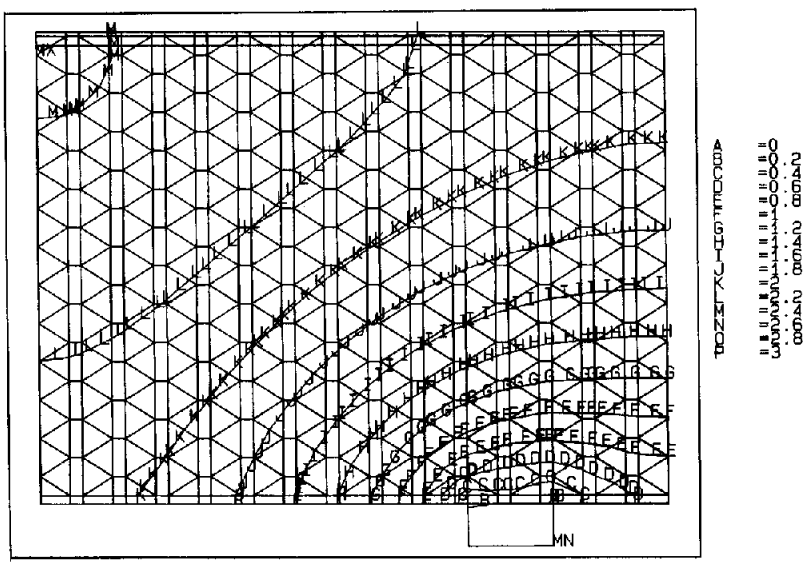

Fig. 8. Potential distribution over the surface of an expanded grid as in Fig. 7, but with the lug shifted towards the centre of the plate.

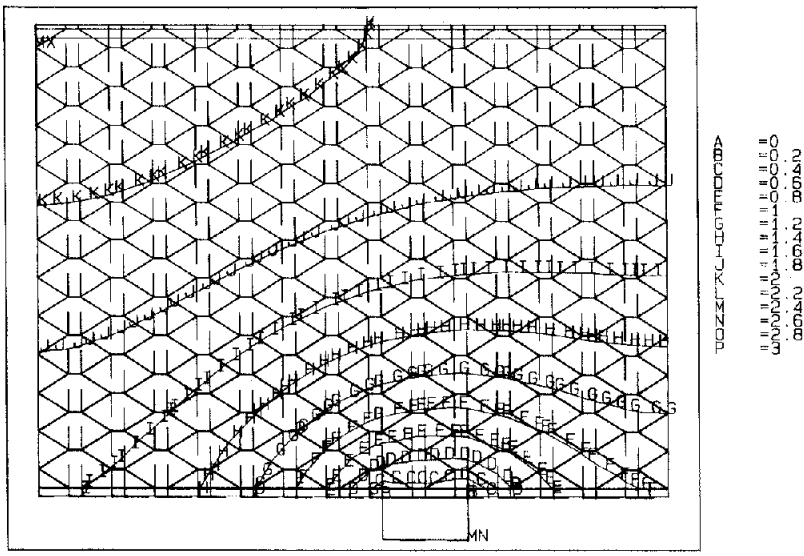

Fig. 9. Potential distribution over the surface of an expanded grid as in Figs. 7 and 8, but with the lug shifted even more towards the centre of the plate.

versa, the amount of lead, which is necessary to achieve a certain grid resistance, is minimized. While in the first case, a battery of same weight and improved performance is obtained, in the latter, the performance is unchanged but the weight is reduced.

Besides the electrical conductivity, grid-design optimization has to take into account several technical criteria. The grid design has to be suited for production. The mechanical strength and the mass-pellet size are both important for the handling of grids and pasted plates. And in case of positive grids, long-term changes in the design through grid corrosion have to be considered: grid design should not be very sensitive with respect to early corrosion, and a faultless manufacturing practice should be possible in order to provide against local corrosion attack at defects of the cast structure.

While these technical aspects have to be considered by the grid designer, and to be tested in practice, the electrical behaviour of a grid under development can be calculated in advance from the CAD drawing alone. FEA and the computer programs designed for this special purpose are a useful tool for improving the design of new grids. The program package enables the designer to test many variants in advance by simulation, before any hardware has to be built. As the program package operates completely as a 'black box' tool, the designer does not need to know the details of this package and especially of the FEA program. Several hypothetical designs can be tested within one hour. The designer successively gains a feeling for advantageous and disadvantageous constructive details. Exotic designs can be tested quickly. Analysis of 'what, where, if...', e.g., 'what will be the performance after a certain degree of corrosion', can be performed easily.

As more variants can be tested by the simulation than by the conventional method, usually more beneficial solutions are found. Furthermore, as only the most promising designs are tested in practice, this approach saves both cost and time.

Acknowledgements

The author is grateful to his colleagues Dr H. Laig-Hörstebrock (VARTA R&D Centre) for detailed introduction to and many helpful discussions on this topic and his own previous work [18], and to Mr A. Hoffmann (VARTA Automotive Battery Division) for his help and engagement to install and to adapt the system to the requirements of practice, and for his numerous suggestions.

References

1 C. Kasper, *Trans. Electrochem. Soc., 77* (1940) 353.
2 C. Kasper, *Trans. Electrochem. Soc., 77* (1940) 365.
3 C. Kasper, *Trans. Electrochem. Soc., 77* (1940) 131.
4 C. Kasper, *Trans. Electrochem. Soc., 78* (1940) 147.
5 C. Kasper, *Trans. Electrochem. Soc., 82* (1940) 153.
6 C. Wagner, *J. Electrochem. Soc., 98* (1951) 116.
7 W. Tobias and R. Wijsman, *J. Electrochem. Soc., 100* (1953) 459.
8 P. M. Robertson, *Electrochim. Acta, 22* (1977) 411.
9 H. Shih and H. W. Pickering, *J. Electrochem. Soc., 134* (1987) 551.
10 M. Matlosz, P.-H. Valloton, A. C. West and D. Landolt, *J. Electrochem. Soc., 139* (1992) 752.
11 J. T. Crennell and F. M. Lea, *J. Inst. Electr. Eng., 66* (1928) 529.
12 C. M. Shepherd, *J. Electrochem. Soc., 112* (1965) 252 and 657.
13 C. M. Shepherd, *J. Electrochem. Soc., 120* (1973) 851.
14 K. Aoki, Y. Nishiki, K. Tokuda and H. Matsuda, *J. Appl. Electrochem., 17* (1987) 552.
15 J. Euler and L. Horn, *Electrochim. Acta, 10* (1965) 1057; *Arch. Elektrotech., 50* (1965) 85.
16 H. Bode and J. Euler, *Naturwissenschaften, 50* (1963) 610; *Electrochim. Acta, 11* (1966) 1211; *11* (1966) 1221; H. Bode, J. Euler, E. Rieder and H. Schmitt, *Electrochim. Acta, 11* (1966) 1231.
17 K. J. Euler, *Arch. Elektrotech., 54* (1971) 122.
18 Entwicklung einer Bleibatterie mit hoher Energie- und Leistungsdichte, *Zuwendungsvertrag BMFT-ET 4046 A, Final Rep.*, VARTA R&D Centre, supported by German Federal Ministery of Research and Technology, 1978.
19 N. E. Bagshaw, K. P. Bromelow and J. Eaton, in D. H. Collins (ed.), *Power Sources 6,* Academic Press, London, 1977, p. 1.
20 J. E. Puzey and W. M. Orriel, in D. H. Collins (ed.), *Power Sources 2,* Academic Press, London, 1968, p. 121.
21 W. Tiedeman, J. Newman and F. DeSua, in D. H. Collins (ed.), *Power Sources 6,* Academic Press, London, 1977, p. 15.
22 W. Tiedeman and J. Newman, *Abstr., Fall Meet. Electrochemical Society,* Pennington, NJ, 1979, No. 169.
23 W. Tiedeman and J. Newman, in S. Gross (ed.), *Proc. Symp. Battery Design and Optimization,* Proc. Vol. 79–1, The Electrochemical Society, Pennington, NJ, 1979, p. 39.
24 W. G. Sunu and B. W. Burrows, *J. Electrochem. Soc., 129* (1982) 688.
25 K. W. Choi and N. P. Yao, in S. Gross (ed.), *Proc. Symp. Battery Design and Optimization,* Proc. Vol. 79–1, The Electrochemical Society, Pennington, NJ, 1979, p. 50.
26 L. E. Vaaler, E. W. Brooman and H. A. Fuggiti, *J. Appl. Electrochem., 12* (1982) 721.
27 Y. Nishiki, K. Aoki, K. Tokuda and H. Matsuda, *J. Appl. Electrochem., 17* (1987) 445.
28 W. G. Sunu and B. W. Burrows, *J. Electrochem. Soc., 128* (1981) 1405.
29 E. C. Dimpault-Darcy, T. V. Nguyen and R. E. White, *J. Electrochem. Soc., 135* (1988) 278.
30 L. E. Vaaler and E. W. Brooman, *Congr. Society Automotive Engineers, Detroit, MI, 1978,* Paper no. 780221.
31 W. G. Sunu and B. W. Burrows, *J. Electrochem. Soc., 131* (1984) 1.

32 K. Asai and T. Hatanaka, *Progr. Batteries Solar Cells, 5* (1984) 201.
33 K. Asai, T. Hatanaka, M. Tsubota, K. Yonezu and K. Ando, *J. Power Sources, 16* (1985) 65.
34 J. Bouet, J. P. Pompon, F. Richard and G. Chedeville, in L. J. Pearce (ed.), *Power Sources 11,* Academic Press, London, 1987, p. 67.
35 Y. Morimoto, Y. Ohya, K. Abe, T. Yoshida and H. Mprimoto, *J. Electrochem. Soc., 135* (1988) 293.
36 L. E. Vaaler, *70th Ann. Meet.,* American Institute of Chemical Engineers, New York, Nov. 1977, Paper no. 99c.
37 J. Meiwes, ETZ *Archiv., 7* (1985) 381.
38 J. Meiwes, ETZ *Archiv., 8* (1986) 79.
39 J. Meiwes, ETZ *Archiv., 8* (1986) 305.
40 J. Meiwes, in *DECHEMA-Monographien,* Vol. 109, VCH Verlagsgesellschaft, Weinheim, 1987, pp. 219–236.
41 J. Meiwes and H.-Ch. Skudelny, *J. Power Sources, 27* (1989) 45.
42 E. M. Valeriote, *J. Power Sources, 28* (1989) 93; E. M. Valeriote, *3rd ILZRO Lead-Acid Battery Seminar, Orlando, FL, May 1989,* pp. 17–64.
43 H. Gu, T. V. Nguyen and R. E. White, *J. Electrochem. Soc., 134* (1987) 2953.
44 H. Gu, T. V. Nguyen and R. E. White, *J. Power Sources, 28* (1992) 206.
45 D. Prengaman, *The Battery Man,* (May) (1982) 16.
46 H. Metzendorf, *J. Power Sources, 7* (1982) 281; *Ph.D. Thesis,* Kassel, 1980.
47 U. B. Thomas, *Trans. Faraday Soc., 94* (1948) 42.
48 J. P. Pohl and W. Schendler, *J. Power Sources, 6* (1981) 245.